Electro-acupuncture alleviates ACE-increased anxiety-like behaviors in mice of adulthood by targeting claustrum D1R^{CaMKII}

Liying Chen[1,2,5], Zhaoyu Liu[1,5], Ziheng Zhao[1,5], Weichao Pan[1], Tao Hu[1], Xiaoyan Wei[1], Jiaxun Nie[1], Feifei Ge[1], Jianhua Ding[3], Yu Fan[1,*], Hee Young Kim[4,*], Xiaowei Guan[1,*]

[1]Department of Human Anatomy and Histoembryology, Nanjing University of Chinese Medicine, Nanjing, China

[2]Department of Critical Care Medicine, Jiangxi Province Hospital of Integrated Chinese and Western Medicine, Nanchang, China

[3]Department of Pharmacology, Nanjing Medical University, Nanjing, China

[4]Department of Physiology, Yonsei University, Seoul, South Korea

[5]These authors equally contribute to this work

Running title: EA treats ACE anxiety by claustrum D1R^{CaMKII}

*Correspondence to: Prof. Xiaowei Guan (guanxw918@njucm.edu.cn), Dr. Yu Fan (yfan@njucm.edu.cn), Prof. Hee Young Kim (vet202001@yuhs.ac)

Phone number: +86-25-85811387

Abstract

Adolescent cocaine exposure (ACE) increases the risk of suffering psychiatric disorders including anxiety in later life, which is a big public health concern with limited treating options. Consistent with our previous study, we found that ACE mice exhibited obvious anxiety-like behaviors in their adulthood, which was efficiently suppressed by electro-acupuncture (EA) at acupoints of Baihui (GV 20) and Yintang (GV 29) with stimulus of a mixed frequency of 2/100 Hz for 28 withdrawal days. In the claustrum (CL) of ACE mice, more CaMKII-positive neurons ($CaMKII^{CL}$) were activated, accompanied with increased expression of dopamine receptor 1 (D1R) on them ($D1R^{CaMKII}$) and phosphorylated-EKR (p-ERK), p-CREB, and BDNF protein levels. Local blockade of CL D1R by SCH23390 or specific knockdown of CL $D1R^{CaMKII}$ by virus suppressed both anxiety-like behaviors and $CaMKII^{CL}$ activity in ACE mice of adulthood, indicating the critical role of CL $D1R^{CaMKII}$ in ACE-enhanced anxiety. Importantly, EA treatment suppressed $CaMKII^{CL}$ activity and $D1R^{CaMKII}$ staining, along with attenuated levels of p-CREB and BDNF in CL of ACE mice. Collectively, our study for the first time identified a novel molecular mechanism of CL $D1R^{CaMKII}$ and $CaMKII^{CL}$ activity in the process of ACE-increased anxiety in adulthood. Further, by targeting CL $D1R^{CaMKII}$, EA at acupoints of GV 20 and GV 29 serves as preventative strategy to adolescent drugs exposure-induced anxiety in the later life.

Keywords: adolescent cocaine exposure, anxiety in adulthood, electro-acupuncture, $CaMKII^{CL}$ activity, $D1R^{CaMKII}$

Significance statement

The current study identifies a novel molecular mechanism of CL $D1R^{CaMKII}$ and $CaMKII^{CL}$ activity in the process of ACE-increased anxiety in adulthood. By targeting CL $D1R^{CaMKII}$, EA at acupoints of GV 20 and GV 29 serves as preventative strategy to adolescent drugs exposure-induced anxiety in the later life.

Introduction

Adolescents presents higher vulnerability to substance abuse (1, 2). Adolescent experience of drug abuse increases risk of developing psychiatric disorders that even persists into adulthood, which is a big public heath concern worldwide (3-8). Previously, we found that adolescent cocaine exposure (ACE) increased anxiety-like behaviors in mice of adulthood (9, 10), which is generally believed as critical factor for driving relapse to drugs in later life (11, 12). Currently, there is few pharmacotherapy options for adolescent substance use-induced anxiety, partially due to serious side-effects caused by anxiolytic medicine. As a non-invasive therapeutic approach, acupuncture has been considered as an efficient intervention on substance use, especially for treatment of the protract abstinence syndrome (such as anxiety) during drug withdrawal period (13-15), but its pharmacological targets remain largely unclear.

The electro-acupuncture (EA), a kind of peripheral acupuncture with electric stimulation, has been shown to improve anxiety without adverse effects (16, 17). Previously, we found that EA at acupoints of Baihui (GV 20) and Yintang (GV 29) during withdrawal period effectively reduced anxiety in ACE mice of adulthood (18). The claustrum (CL) is a thin stripped nucleus situated between the insular cortex and striatum, which is composed by 90 percent of CaMKII-positive glutamatergic neurons ($CaMKII^{CL}$) (19, 20). In marijuana addicts (21, 22) and internet game addicts (23), the CL exhibited greater activity than controls. Recently, Terem et al. (24) found that the CL receives dopamine inputs and expresses dopamine D1 receptors (D1R), and claustral D1R-positive cells is required for acquisition of cocaine preference. Further, activation of CL elicited, whereas silencing of the CL attenuated the anxiety-related behaviors in animal models of acute social defeat stress (25). Collectively, these studies demonstrate the critical role of CL activity in the process of addiction and anxiety. Early in 2006, Shapo et al. (26) reported that acupuncture at Weizhong points could significantly evoke CL activity in humans. Whether CL is the key target for EA to treat ACE-related anxiety, and what is the underlying molecular mechanism, is still unknown.

In the present study, male mice were exposed to cocaine during adolescence from postnatal day 28 (P28) to P42 (27). When the mice grew up to adult age, the role of CL D1R^{CaMKII} and the effect of EA at GV 20 and GV 29 in the process of ACE-induced anxiety in mice of adulthood.

Results

ACE enhances the anxiety-like behaviors, triggers CaMKII^{CL} activation and increases CL D1R^{CaMKII} levels in mice of adulthood

To examine anxiety-like behaviors, mice were subjected to behavioral tests of EPM, OFT and MBT in their adulthood (Figure 1A). As shown in Figure 1B, ACE mice of adulthood exhibited less time spent (n = 24, t = 2.292, p = 0.0319) and less entries (n = 24, t = 2.120, p = 0.0455) into the open arms, but similar the distances traveled in open arms of the EPM apparatus (n = 24, t = 1.497, p = 0.1486) than those of adolescent saline exposure (ASE) mice of adulthood. During the OFT (Figure 1C), ACE mice spent less time (n = 24, t = 2.308, p = 0.0308) in the central area of box, while had similar entries (n = 24, t = 1.488, p = 0.1509) into the central area and total distances traveled (n = 24, t = 0.008965, p = 0.9929) in the OFT box than ASE controls. In the MBT, the buried beads by ACE mice had no significant difference at each time point (n = 24, $F_{(6,132)}$ = 0.3929， p = 0.8826) and in total (n = 24, t = 0.8578, p = 0.4003) when compared to ASE controls (Figure S1A).

The c-Fos and CaMKII were used as markers to detect the neuronal activity and glutamatergic neurons, respectively. The total protein level of c-Fos (n = 6, t = 2.811, p = 0.0483) was higher in ACE than in ASE mice of adulthood (Figure 1D). Both the percentage (n = 11, t = 2.466, p = 0.0358) and number (n = 11, t = 3.106, p = 0.0126) of c-Fos-positive CaMKII^{CL} neurons were higher in ACE mice than those in ASE mice of adulthood (Figure 1E).

On CaMKII^{CL} neurons, the expression of D1R (D1R^{CaMKII}) was much higher (n = 6, t = 3.177, p = 0.0336) in ACE than in ASE mice of adulthood (Figure 1F). The total levels of mRNA (Figure 1G) and protein (Figure 1H) of CL D1R (mRNA, n = 9, t = 2.583, p = 0.0363; protein, n = 6, t = 7.389, p = 0.0018) was higher, but not that of D2R (mRNA, n = 11, t = 0.2676, p = 0.7950; protein, n = 6, t = 0.1621, p = 0.8791) and D3R (mRNA, n = 11, t = 0.3458, p = 0.7374; protein, n

= 6, t = 1.159, p = 0.2035) in ACE than in ASE mice of adulthood. In parallel, the protein levels of p-$ERK_{1/2}$ (n = 6, t = 4.905, p = 0.0080), ratio of p-$ERK_{1/2}$ to $ERK_{1/2}$ (n = 6, t = 3.239, p = 0.0317), p-CREB (n = 6, t = 5.871, p = 0.0042), p-CREB/ CREB (n = 6, t = 3.502, p = 0.0248) and BDNF (n = 6, t = 2.940, p = 0.0424) were higher in ACE group mice than controls, but that of $ERK_{1/2}$ (n = 6, t = 0.9475, p = 0.3970) and CREB (n = 6, t = 0.4336, p = 0.6869) had no significant difference between ACE and ASE mice of adulthood (Figure 1I, 1J).

Specific antagonistic CL D1R suppresses anxiety-like behaviors and attenuates $CaMKII^{CL}$ activation in ACE mice of adulthood

To evaluate the role of CL D1R in ACE-induced anxiety, the selective D1R antagonist SCH-23390 was bilaterally injected into local CL 20 min prior to the tests of EPM, OFT and NSFT (Figure 2A). Compared with vehicle-treated mice, local SCH-23390 treatment significantly enhanced the time spent in open arms (n = 19, t = 2.322, p = 0.0329), and did not affect the entries into the open arms (n = 19, t = 1.085, p = 0.2930) and the distances traveled in open arms of EPM apparatus (n = 19, t = 0.5363, p = 0.5987) in ACE mice of adulthood (Figure 2B). SCH-23390 treatment had no influence in the time spent (n = 19, t = 1.688, p = 0.1096), the entries (n = 19, t = 1.105, p = 0.2847) in the central area, and the total distances traveled by ACE mice (n = 19, t = 1.676, p = 0.1121) in the OFT box, when compared with the vehicle-treated mice (Figure 2C). Similarly, there is no difference on the latency (n = 19, t = 0.6239, p = 0.5410) and intake (n = 19, t = 0.9492, p = 0.3558) of feeding in the NSFT between vehicle-treated and SCH-23390-treated ACE mice (Figure 2D).

As shown in Figure 2E, local SCH-23390 treatment significantly attenuated the percentage of c-Fos-positive $CaMKII^{CL}$ neurons (n = 12, t = 3.097, p = 0.0113), when compared with vehicle-treated mice.

Specific knockdown of CL $D1R^{CaMKII}$ inhibits anxiety-like behaviors and attenuates $CaMKII^{CL}$ activation in ACE of adulthood

Specific knockdown of $D1R^{CaMKII}$ on $CaMKII^{CL}$ neurons were performed in ACE mice of adulthood (Figure 3A). Adeno-associated virus of *CaMKIIap-EGFP-MIR155(shDrd1)-SV40 PolyA* (ACE_{KD}) and *CaMKIIap-EGFP-MIR155(MCS)-SV40 PolyA* and *AAV9-CON540* (ACE_{Ctrl}) were bilaterally infused into CL, and

about 55% CaMKII-positive neurons within CL were transfected with virus (Figure 3B). Compared with ACE_{Ctrl} mice, the levels of D1R protein (n = 6, t = 3.465, p = 0.0257, Figure 3C) was decreased in CL of ACE_{KD} mice.

ACE_{KD} mice exhibited more time spent (n = 16, t = 2.152, p = 0.0493), and did not affect the entries into the open arms (n = 16, t = 1.134, p = 0.2759), and similar distance traveled (n = 16, t = 1.831, p = 0.0885) in the EPM apparatus, when compared with ACE_{Ctrl} mice (Figure 3D). There were no differences on the time spent in central area (n = 16, t = 1.500, p = 0.1559), the entries (n = 16, t = 0.1574, p = 0.8772) in the central area, the total distances traveled by ACE mice (n = 16, t = 0.1926, p = 0.8500) in the OFT box (Figure 3E). Moreover, the latency (n = 16, t = 0.02965, p = 0.9768) and intake (n = 16, t = 1.088, p = 0.2950) of feeding did not change in the NSFT (Figure 3F) between ACE_{KD} and ACE_{Ctrl} mice. In parallel, the percentage of c-Fos-positive $CaMKII^{CL}$ neurons was much lower (n = 6, t = 3.207, p = 0.0327) in ACE_{KD} mice than that in ACE_{Ctrl} mice (Figure 3G).

EA treatment alleviates anxiety-like behaviors, rescues both $CaMKII^{CL}$ activity and CL $D1R^{CaMKII}$ levels in ACE mice of adulthood

EA treatments at acupoints of GV20 and GV29 during P42-P70 were carried out in ACE mice (ACE_{EA}), and placebo acupoints were used as sham EA treatment (ACE_{SEA}) (Figure 4A). Compared with ACE_{SEA} mice, ACE_{EA} mice spent more time (n = 23, t = 2.084, p = 0.0496), similar entries into the open arms (n = 23, t = 1.536, p = 0.1394) and similar the distances traveled in open arms of the EPM apparatus (n = 23, t = 1.186, p = 0.0837, Figure 4B). There were no differences in the time spent (n = 23, t = 0.1918, p = 0.8498), the entries (n = 23, t = 0.08086, p = 0.9363) into the central area and the total distances traveled (n = 23, t = 0.3799, p = 0.7078) in the OFT box between ACE_{EA} and ACE_{SEA} mice (Figure 4C). In the NSFT (Figure 4D), ACE_{EA} mice intake more food (n = 23, t = 2.532, p = 0.0194), and spent similar latency of feeding (n = 23, t = 0.6190, p = 0.5426), when compared with ACE_{SEA} mice.

Compared with ACE_{SEA} mice, both the percentage (n = 12, t = 4.246, p = 0.0017) and the number (n = 12, t = 3.076, p = 0.0117) of c-Fos-positive $CaMKII^{CL}$ neurons were much lower in ACE_{EA} mice (Figure 4E). In parallel, both

levels of total D1R protein in CL (n = 6, t = 4.396, p = 0.0117, Figure 4F) and $D1R^{CaMKII}$ staining (n = 6, t = 4.874, p = 0.0082, Figure 4G) were lower in ACE_{EA} mice than that in ACE_{SEA} mice.

As shown in Figure 4H-I, there were no differences on protein levels p-$ERK_{1/2}$ (n = 6, t = 0.2242, p = 0.8336), $ERK_{1/2}$ (n = 6, t = 0.7388, p = 0.5010), CREB (n = 6, t = 0.9656 p = 0.3889) and ratio of p-$ERK_{1/2}$ to $ERK_{1/2}$ (n = 6, t = 0.3008, p = 0.7786) in CL between ACE_{EA} and ACE_{SEA} mice. While, the levels of p-CREB (n = 6, t = 4.464, p = 0.0111), BDNF (n = 6, t = 2.957, p = 0.0417) and radio of p-CREB to CREB (n = 6, t = 3.191, p = 0.0332) were lower in ACE_{EA} mice, when compared with ACE_{SEA} mice.

Discussion

Consistent with our previous finding (18), we found that ACE mice exhibited obvious anxiety-like behaviors in their adulthood, which was efficiently suppressed by electro-acupuncture (EA) at acupoints of Baihui (GV 20) and Yintang (GV 29) during withdrawal days. In parallel, ACE activated more CaMKII-positive neurons in CL ($CaMKII^{CL}$) and increased D1R expression on $CaMKII^{CL}$ (D1R), accompanied by increased protein levels of p-EKR, p-CREB and BDNF in the CL. Local blockade of CL D1R by SCH23390 or specific knockdown of CL $D1R^{CaMKII}$ by virus suppressed both anxiety-like behaviors and $CaMKII^{CL}$ activity in ACE mice of adulthood, indicating the critical role of CL $D1R^{CaMKII}$ in ACE-enhanced anxiety. Importantly, EA treatment suppressed $CaMKII^{CL}$ activity and $D1R^{CaMKII}$ staining, along with attenuated levels of p-CREB and BDNF in CL of ACE mice.

Drug abuse such as cocaine during adolescence, a sensitive period of heightened propensity to substance use in humans, enhance risk of developing psychiatric disorders, which even persist into adulthood (2, 10, 28). Consistent with human and animal studies on ACE (9, 18, 29, 30), ACE mice exhibited more anxiety in their adulthood here. Moreover, we found that $CaMKII^{CL}$ activity was involved in the process of anxiety in ACE mice. Recently, Niu et.al (25) reported that CL is crucial for the control of stress-induced anxiety, as indicated by the attenuated social defeat stress-induced anxiety with silencing of the $CaMKII^{CL}$. In addition, the CL receives input from other anxiety related brain

regions and sends axonal outputs to the prefrontal cortex (PFC) (31, 32), suggesting a possible role of CL in modulation of anxiety. In our previous study, we found that ACE-heightened function of mPFC GABAergic transmission was likely mediates ACE-related anxiety in adult mice (9). In the future study, the role of neural circuits of CL-PFC in ACE-related anxiety would be explored. DA receptors (DRs) are metabotropic G protein-coupled receptors that include two different classes: D1-like receptor subfamily (D1R and D5R) and D2-like receptor subfamily (D2R, D3R, and D4R) (33, 34). There contains a high to moderate amount of D1R and D2R in the CL (24, 35-39). A recent study by Terem et al. (24) demonstrated that CL D1R-expressing neurons were activated by cocaine administration. Here, we found that ACE increased mRNA and protein levels of D1R rather than D2R and D3R in the CL. Moreover, local administration of D1R-specific antagonist in CL or specific knockdown of $D1R^{CaMKII}$ of CL could increase the time spent in open arms of EPM and decreased $CaMKII^{CL}$ activity, indicating the critical role of $D1R^{CaMKII}$-$CaMKII^{CL}$ activity in ACE anxiety. At present, few studies focus on the potential molecules that underly the regulation of CL $D1R^{CaMKII}$ on $CaMKII^{CL}$ activity. The ERK, CREB and BDNF are well-studied downstream molecules of D1R, including substance use and anxiety. In other D1R-rich brain regions, such as PFC and hippocampus, cocaine abuse could alter p-ERK (40), p-CREB (41) and BDNF (42, 43). Here, we found that protein levels of p-ERK, p-CREB and BDNF were significantly increased in CL of ACE mice, suggesting a possible downstream regulator of p-ERK, p-CREB and BDNF for CL $D1R^{CaMKII}$ in the process of ACE-induced anxiety.

Electro-acupuncture (EA) has been widely applied in management of substance abuse, especially for drugs-caused withdrawal symptoms, including anxiety (17, 18, 44). Consistent with our previous study (18), EA at acupoints of GV20 and GV29 alleviated the anxiety in ACE mice of adulthood, but the pharmacological targets remain unknown. Shao et al (45) reported that EA at Zusanli (ST36)and Kunlun(BL60) could reduce anxiety-like behaviors in animals by suppressing neuropeptide Y in anterior cingulate cortex. Recently, Wu et al. (46) found that EA at ST36 and Sanyinjiao (SP6) alleviated anxiety by activating D1R or antagonizing D2R in the basolateral amygdala. Here, we

found that EA at GV20 and GV29 reversed ACE-enhanced $CaMKII^{CL}$ activity and CL $D1R^{CaMKII}$, indicating a potential targets of CL $D1R^{CaMKII}$-$CaMKII^{CL}$ activity for EA to treat ACE-induced anxiety. To our knowledge, we provide the first piece of evidence to identify the role of CL in the process of ACE-induced anxiety and in the anxiolytic effects of EA in ACE mice. Further, we found that EA reversed ACE-increased p-CREB and BDNF levels in CL.

In conclusion, our findings revealed a novel molecular mechanism of CL $D1R^{CaMKII}$ and $CaMKII^{CL}$ activity in the process of ACE-related anxiety in mice of adulthood. By targeting CL $D1R^{CaMKII}$, EA treatment efficiently suppressed anxiety in ACE mice of adulthood.

Materials and methods

Animals

Male C57BL/6 wild type (WT) mice weighing 12-16 g were used. All animals were housed at constant humidity (40~60%) and temperature (24 ± 2ºC) with a 12-hour light/dark cycle (lights on at 8 a.m.) and allowed free access to food and water. Handling of the animals was carried out for three days before onset of experiments. All procedures were carried out in accordance with the National Institutes of Health Guide for the Care and Use of Laboratory Animals and approved by the Institutional Animal Care and Use Committee (IACUC) at Nanjing University of Chinese Medicine.

Drug treatment

On postnatal day 28 (P28), male C57BL/6 WT mice were assigned to receive a single daily injection of cocaine hydrochloride (15 mg/kg, dissolved in saline, i.p., Qinghai Pharmaceutical, China) or saline (0.2 mL, i.p.) once daily at 10 a.m. for 14 consecutive days. From P42-P70, these mice were kept at their home cage (four mice one cage). On P71、P73 and P75, the related behavioral tests were performed. On P79, the mice were sacrificed after stimulus of elevated plus maze (EPM) procedure. The brain tissue was collected for qPCR, western blot and immunofluorescence.

Electro-acupuncture treatment

During P42 to P70, two acupuncture needles (0.16 × 7 mm, Hwato, China) were inserted gently in a depth of 2–3 mm at the acupoints of GV20 (Baihui, the

midpoint between the auricular apices) and GV29 (Yintang, the midpoint between the medial ends of the two eyebrows) in each mouse, the acupoints were electric stimuli of 2/100 Hz at an intensity of 1 mA (HANS Electronic Apparatus, China) for 30 minutes once a day at acupoints of GV20 and GV29 in EA mice, while at "placebo-point" (at 1 cm from base of the tail) in Sham EA mice (SEA, Figure S2A).

Behavioral tests

Elevated plus maze (EPM), open field test (OFT), marble burying test (MBT) and novelty suppressed feeding test (NSFT) were performed to assess anxiety-like behaviors. All behavioral tests were conducted during light cycle. In the current study, four separated cohorts of the adolescent cocaine exposure mice were used to assess anxiety-like behaviors. All data were recorded and analyzed by TopScan H system (TopScan, USA). The mice were kept at their home cage until experiments.

The EPM apparatus (TopScan, Kansas City, MO, USA) consists of 4 elevated arms (52 cm above the floor) arranged in a cross pattern with two 1-cm walled arms (open arms) and two 40-cm walled arms (closed arms). Each mouse was placed in the center portion of the EPM with its head facing an open arm and allowed freely to explore the maze for 5 min. The time spent, the entries and the distance traveled in the open arms were recorded.

In OFT, mice were placed gently in the center of the open field apparatus (50 × 50 × 50 cm) individually, and the time spent and the entries into the central area (16× 16 × 16 cm) of the box and the total distance traveled in the box were recorded for 5 min with a camera positioned overhead.

In MBT, mice were placed individually in a clean cage (25 × 25 × 50 cm) with 5 cm corncob bedding. Sixteen marbles (14 mm diameter) were distributed evenly in the cages in four rows of four on top of cage bedding. Mice were left undisturbed for 30 minutes, and the number of marbles buried (>50% of marble covered by bedding material) was recorded.

In NSFT, mice were placed in a square acrylic box (50 × 50 × 50 cm) with the floor covered by 3 cm of corncob bedding. Twenty-four hours before the test, all animals were food deprived. On the day of the test a single regular chow

pellet was placed in a white platform located in the middle of the box. Each animal was placed in one of the apparatus corners, and the latency to start feeding in the new environment was measured with a cutoff period of 5 minutes. The stopwatch was immediately stopped when the mouse bit the chow, using its forepaws sitting on its haunches. After the test, all animals returned to their home cages, and the amount of food consumed in a total period of 5 minutes was measured.

Western blot

Total protein was extracted from mice CL (the middle region) using RIPA lysis buffer (Beijing ComWin Biotech Co., China) according to the manufacturer's instructions. Protein samples (15 μg) was separated by 10% SDS–PAGE, 12% SDS–PAGE and electrophoretically transferred onto PVDF membranes. The transferred membranes were blocked with 5% non-fat dry milk or 5% BCA and 0.1% Tween 20 in 10 mM Tris–HCl (TBST buffer, pH 7.5) for 1.5 h at room temperature, then subsequently incubated with the following primary antibodies: D1R (1:1000, Rabbit, RRID:AB_10598308, Proteintech, USA), D2R (1:1000, Rabbit, ER1907-70, Hua An Biotechnology Company, China), D3R (1:1000, Mouse, ab155098, Abcam, UK), $ERK_{1/2}$ (1:1000, Rabbit, BM4326, Boster, China), p-$ERK_{1/2}$ (1:1000, Rabbit, BM4326, Boster, China), CREB (1:1000, Rabbit, RRID:AB_10699020, Cell Signaling Technology, USA), p-CREB (1:1000, Rabbit, RRID:AB_2561044, Cell Signaling Technology, USA), c-Fos (1:2000, Rabbit, RRID:AB_2247211, Cell Signaling Technology, USA), BDNF (1:1000, Mouse, RRID:AB_2881675, Proteintech, USA). The next day, the membranes were washed three times in Tris-buffered saline with Tween 20 (TBS-T) and incubated with horseradish peroxidase (HRP)-conjugated secondary antibody goat anti-rabbit or goat anti mouse (1:5000, Beijing ComWin Biotech Co., China) at room temperature for 1 h. The blots were visualized by the ECL kit (Beyotime, China) and the signal was visualized by imaging system (Tanon-5200, Shanghai, China). The blots were washed with stripping buffer (Beyotime Institute of Biotechnology) to allow reprobing with other antibodies. In this study, GAPDH or β-actin was used as the loading control. Values for target protein levels were calculated using Image J software

(NIH, USA). The relative level of each protein expression (blot volume) was normalized to GAPDH or β-actin.

RNA extraction and quantitative real-time PCR

Mice were decapitated 45 min following EPM behavioral tests on P79. CL were collected immediately. Total RNA was extracted from the middle of CL using FastPure Cell/Tissue Total RNA Isolation Kit (Vazyme, China), according to the manufacturer's instructions. All samples were tested for concentration and purified using a 4200 TapeStation (Agilent Technologies, Santa Clara, USA). After RNA extraction, the amount of RNA was normalized across samples, and cDNA was created using iScript (1708891, Bio-Rad, Hercules, USA). Actin was used as the internal control. The primers of *D1R, D2R*, *D3R* and Actin were as follows: *D1R* (forward, ATGGCTCCTAACACTTCTACCA; reverse, GGGTATTCCCTAAGAGAGTGGAC); *D2R* (forward, ACCTGTCCTGGTACGATGATG; reverse, GCATGGCATAGTAGTTGTAGTGG); *D3R* (forward, AGACAACATGGAGAGCTGAAACGCT; reverse, TTCAGGGCTGTGGATAACCTGCC); Actin (forward, GGCTGTATTCCCCTCCATCG; reverse, CCAGTTGGTAACAATGCCATGT). *D1R*, *D2R* and *D3R* mRNA levels were normalized to Actin mRNA levels. The relative mRNA level was calculated by the comparative CT method ($2^{-\Delta\Delta Ct}$).

Immunofluorescence

Mice brains were collected within 90 min after EPM procedure and perfused with 4% paraformaldehyde (PFA). The coronal brain sections (30 μm) were cut on a cryostat (Leica, Germany). The sections were incubated in 0.3% (v/v) Triton X-100 for 0.5 h, blocked with 5% donkey serum for 1.5 h at room temperature, and incubated overnight at 4°C with the following primary antibodies: rabbit anti-c-Fos (1:2000, RRID: AB_2247211, Cell Signalling Technology, USA) , mouse anti-NeuN (1:800, RRID: AB_2298772, Millipore, USA), mouse anti-GAD67 (1:800, RRID: AB_2278725, Millipore, USA), mouse anti-PV (1:250, BM1339, Boster Biotechnology, China), mouse anti-SOM (1:50, RRID: AB_2271061, Santa Cruz, USA) and mouse anti-CaMKIIα (1:100, RRID: AB_626789, Santa Cruz, USA), followed by the corresponding fluorophore-conjugated secondary antibodies for 1 h at room temperature. The following

secondary antibodies were used here: Alexa Fluor 555-labeled donkey anti-rabbit secondary antibody (1:500, RRID: AB_162543, Invitrogen, USA), Alexa Fluor 488-labeled donkey anti-mouse secondary antibody (1:500, RRID: AB_141607, Invitrogen, USA). Fluorescence signals were visualized using a Leica DM6B upright digital research microscope (Leica, Germany) or Leica TCS SP8 (Leica, Germany).

Local administration of SCH-23390 in CL

The cannula (O.D. 0.41 mm, C.C 3.0 mm, Cat 62004, RWD, China) were planted into CL (AP + 0.75 mm, ML ± 3.30 mm, DV – 2.50 mm) of ACE mice on PD64 before anxiety-like behaviors test. After surgery, mice were maintained at home cage about 1 week. From PD71, mice were subjected to EPM, OFT, NSFT. The D1 receptor antagonist R(+)-7-chloro-8-hydroxy-3-methyl-1-phenyl-2,3,4,5-tetrahydro-1H-3-benzazepine hydrochloride (SCH-23390, Selleck chemicals, China) was dissolved in 0.9% saline and stored -80°C. A volume of 70 nL of SCH-23390 were bilaterally injected into CL at a rate of 10 nL/min at 20 min prior to behavioral tests.

Specific knockdown of D1R On CaMKII^{CL} neurons

On PD50, mice were anesthetized with 2% isoflurane in oxygen, and were fixed in a stereotactic frame (RWD, Shenzhen, China). A heating pad was used to maintain the core body temperature of the mice at 36°C. The coordinates of CL were defined as AP + 0.62 mm, ML ± 3.05 mm, DV –3.50 mm. A volume of 70 nL virus of *CaMKIIap-EGFP-MIR155(shDrd1)-SV40 PolyA* (KD group, Titer: 8.89E+13v.g/ml, GeneChem, Shanghai, China) and *CaMKIIap-EGFP-MIR155(MCS)-SV40 PolyA* (Ctrl group, Titer: 1E+13v.g/ml, GeneChem, Shanghai, China) were injected bilaterally into CL at a rate of 10 nL/min. After surgery, mice were kept at home-cage about 3 weeks.

Statistical analysis

Statistical analysis was carried out using GraphPad Prism 8.0.2 software. Data are presented as the Mean ± SEM. The MBT results was analyzed by Two-Way ANOVA followed by Šídák's multiple comparisons test. Other data was analyzed by unpaired *t*-tests. Statistical significance was set as $p < 0.05$.

Author contribution

Chen L, Liu Z and Zhao Z have equal contribution to the manuscript. Chen L, Liu Z and Zhao Z performed behavioral tests, morphological tests and virus-related experiment. Pan W, Hu T, Wei X and Nie J assist the experiment. Fan Y, Ge F and Ding J performed data analysis. Guan X and Fan Y wrote the manuscript. Kim HY edited the manuscript. Guan X developed the overall concept.

Acknowledgment

This work is supported by National Natural Science Foundation of China (82211540400, 82271531 and 82071495), Natural Science Foundation of Jiangsu Province, China (BK20201398) and Natural Science Foundation of the Higher Education Institutions of Jiangsu Province, China (21KJB360007).

Conflict of interests

The authors have no conflict of interests to declare.

Data availability statement

The data that support the findings of this study are available from the corresponding author upon reasonable request.

Reference

1. Laviola G, et al. Psychobiological risk factors for vulnerability to psychostimulants in human adolescents and animal models. *Neuroscience and biobehavioral reviews.* 1999;23(7):993-1010.
2. Chambers RA, et al. Developmental neurocircuitry of motivation in adolescence: a critical period of addiction vulnerability. *The American journal of psychiatry.* 2003;160(6):1041-52.
3. Salmanzadeh H, et al. Adolescent drug exposure: A review of evidence for the development of persistent changes in brain function. *Brain research bulletin.* 2020;156(105-17.
4. Bis-Humbert C, and García-Fuster MJ. Adolescent cocaine induced persistent negative affect in female rats exposed to early-life stress. *Psychopharmacology.* 2021;238(12):3399-410.
5. Rice J, et al. Region-specific interneuron demyelination and heightened anxiety-like behavior induced by adolescent binge alcohol treatment. *Acta neuropathologica communications.* 2019;7(1):173.
6. Moss HB, et al. Early adolescent patterns of alcohol, cigarettes, and marijuana polysubstance use and young adult substance use outcomes in a nationally representative sample. *Drug and alcohol dependence.* 2014;136(51-62.
7. Hanson KL, et al. Changes in neuropsychological functioning over 10 years following adolescent substance abuse treatment. *Psychology of addictive behaviors : journal of the Society of Psychologists in Addictive Behaviors.* 2011;25(1):127-42.
8. Rutherford HJ, et al. Neurobiology of adolescent substance use disorders: implications for prevention and treatment. *Child and adolescent psychiatric clinics of North America.* 2010;19(3):479-92.
9. Shi P, et al. Adolescent cocaine exposure enhances the GABAergic transmission in the prelimbic cortex of adult mice. *FASEB journal : official publication of the Federation of American Societies for Experimental Biology.* 2019;33(7):8614-22.
10. Zhu W, et al. Adolescent cocaine exposure induces prolonged synaptic modifications in medial prefrontal cortex of adult rats. *Brain structure & function.* 2018;223(4):1829-38.
11. Stopponi S, et al. Chronic THC during adolescence increases the vulnerability to stress-induced relapse to heroin seeking in adult rats. *European neuropsychopharmacology : the journal of the European College of Neuropsychopharmacology.* 2014;24(7):1037-45.
12. Erb S. Evaluation of the relationship between anxiety during withdrawal and stress-induced reinstatement of cocaine seeking. *Progress in neuro-psychopharmacology & biological psychiatry.* 2010;34(5):798-807.
13. Kim DH, et al. Effects of acupuncture on the anxiety-like behavior induced by withdrawal from chronic morphine use. *Neuroscience letters.* 2018;664(38-42.
14. Chae Y, et al. Effect of acupuncture on anxiety-like behavior during nicotine withdrawal and relevant mechanisms. *Neuroscience letters.* 2008;430(2):98-102.
15. Pilkington K. Acupuncture therapy for psychiatric illness. *International review of neurobiology.* 2013;111(197-216.

16. Amorim D, et al. Acupuncture and electroacupuncture for anxiety disorders: A systematic review of the clinical research. *Complementary therapies in clinical practice.* 2018;31(31-7.
17. Zeng L, et al. Electro-acupuncture improves psychiatric symptoms, anxiety and depression in methamphetamine addicts during abstinence: A randomized controlled trial. *Medicine.* 2018;97(34):e11905.
18. Nie J, et al. Electro-acupuncture alleviates adolescent cocaine exposure-enhanced anxiety-like behaviors in adult mice by attenuating the activities of PV interneurons in PrL. *FASEB journal : official publication of the Federation of American Societies for Experimental Biology.* 2020;34(9):11913-24.
19. Hinova-Palova DV, et al. Topographical distribution and morphology of NADPH-diaphorase-stained neurons in the human claustrum. *Frontiers in systems neuroscience.* 2014;8(96.
20. Druga R, et al. The Claustrum: Structural, Functional, and Clinical Neuroscience. *The Claustrum: Structural, Functional and Clinical Neuroscience, eds Smythies J R, Edelstein L R, Ramachandran V S* 2014:29-84.
21. Yanes JA, et al. Neuroimaging meta-analysis of cannabis use studies reveals convergent functional alterations in brain regions supporting cognitive control and reward processing. *Journal of Psychopharmacology.* 2018;32(3):283-95.
22. Acheson A, et al. Functional activation and effective connectivity differences in adolescent marijuana users performing a simulated gambling task. *Journal of addiction.* 2015;2015(783106.
23. Zarrindast MR, and Khakpai F. The Modulatory Role of Dopamine in Anxiety-like Behavior. *Archives of Iranian medicine.* 2015;18(9):591-603.
24. Terem A, et al. Claustral Neurons Projecting to Frontal Cortex Mediate Contextual Association of Reward. *Current biology : CB.* 2020;30(18):3522-32.e6.
25. Niu M, et al. Claustrum mediates bidirectional and reversible control of stress-induced anxiety responses. *Science advances.* 2022;8(11):eabi6375.
26. Shapo GR, et al. [Effects of acupuncture at Weizhong (BL40) on brain function with PET/CT]. *Zhongguo Zhong xi yi jie he za zhi Zhongguo Zhongxiyi jiehe zazhi = Chinese journal of integrated traditional and Western medicine.* 2006;26(11):969-72.
27. Spear LP. The adolescent brain and age-related behavioral manifestations. *Neuroscience and biobehavioral reviews.* 2000;24(4):417-63.
28. Caffino L, et al. The effects of cocaine exposure in adolescence: Behavioural effects and neuroplastic mechanisms in experimental models. *British journal of pharmacology.* 2021;179(17).
29. Estelles J, et al. Cocaine exposure during adolescence affects anxiety in adult mice. *Brain research bulletin.* 2007;71(4):393-403.
30. Lopez B, et al. Anxiety and risk for substance dependence among late adolescents/young adults. *Journal of anxiety disorders.* 2005;19(3):275-94.
31. Jackson J, et al. Inhibitory Control of Prefrontal Cortex by the Claustrum. *Neuron.* 2018;99(5):1029-39.e4.
32. Zingg B, et al. Input-output organization of the mouse claustrum. *The Journal of comparative neurology.* 2018;526(15):2428-43.

33. Klein MO, et al. Dopamine: Functions, Signaling, and Association with Neurological Diseases. *Cellular and molecular neurobiology.* 2019;39(1):31-59.
34. Beaulieu JM, and Gainetdinov RR. The physiology, signaling, and pharmacology of dopamine receptors. *Pharmacological reviews.* 2011;63(1):182-217.
35. Camps M, et al. Autoradiographic localization of dopamine D 1 and D 2 receptors in the brain of several mammalian species. *Journal of neural transmission General section.* 1990;80(2):105-27.
36. Hasbi A, et al. Dopamine D1-D2 receptor heteromer expression in key brain regions of rat and higher species: Upregulation in rat striatum after cocaine administration. *Neurobiology of disease.* 2020;143(105017.
37. Borroto-Escuela DO, and Fuxe K. On the G Protein-Coupled Receptor Neuromodulation of the Claustrum. *Neurochemical research.* 2020;45(1):5-15.
38. Hall H, et al. Autoradiographic localization of extrastriatal D2-dopamine receptors in the human brain using [125I]epidepride. *Synapse.* 1996;23(2):115-23.
39. Meador-Woodruff JH, et al. Distribution of D2 dopamine receptor mRNA in the primate brain. *Progress in neuro-psychopharmacology & biological psychiatry.* 1991;15(6):885-93.
40. Siemsen BM, et al. Intra-prelimbic cortical inhibition of striatal-enriched tyrosine phosphatase suppresses cocaine seeking in rats. *Addiction biology.* 2018;23(1):219-29.
41. Valzachi MC, et al. Enhancement of Behavioral Sensitization, Anxiety-Like Behavior, and Hippocampal and Frontal Cortical CREB Levels Following Cocaine Abstinence in Mice Exposed to Cocaine during Adolescence. *PloS one.* 2013;8(10):e78317.
42. Caffino L, et al. Repeated cocaine exposure dysregulates BDNF expression and signaling in the mesocorticolimbic pathway of the adolescent rat. *The world journal of biological psychiatry : the official journal of the World Federation of Societies of Biological Psychiatry.* 2019;20(7):531-44.
43. Caffino L, et al. Anhedonic-like behavior and BDNF dysregulation following a single injection of cocaine during adolescence. *Neuropharmacology.* 2020;175(108161.
44. Kim DH, et al. Effects of acupuncture on the anxiety-like behavior induced by withdrawal from chronic morphine use. *Neuroscience letters.* 2018;664(38-42.
45. Shao F, et al. Electroacupuncture Alleviates Anxiety-like Behavior in Pain Aversion Rats by Attenuating the Expression of Neuropeptide Y in Anterior Cingulate Cortex. *Clinical Complementary Medicine and Pharmacology.* 2022;2(2):100019.
46. Wu M, et al. Electroacupuncture Alleviates Anxiety-Like Behaviors Induced by Chronic Neuropathic Pain via Regulating Different Dopamine Receptors of the Basolateral Amygdala. *Molecular neurobiology.* 2022.

Figure legends

Figure 1. ACE enhances the anxiety-like behaviors, triggers CaMKII^{CL} activation and increases CL D1R^{CaMKII} levels in mice of adulthood. A, Experimental timeline. **B**, EPM test. **C**, OFT. **D**, Total protein levels of c-Fos in CL. **E**, The percentage and number of c-Fos-positive CaMKII^{CL} neurons. Scale bar, 300 μm/50 μm. **F,** The expression of D1R^{CaMKII}. Scale bar, 200 μm/50 μm. **G**, The *D1R, D2R and D3R* mRNA levels in CL. **H,** The D1R, D2R and D3R protein levels in CL. **I,** Levels of p-ERK$_{1/2}$ and ERK$_{1/2}$ in CL. **J,** Levels of p-CREB, CREB and BDNF in CL. ASE, adolescent saline exposure; ACE, adolescent cocaine exposure. N.S., $p > 0.05$, *, $p < 0.05$, **, $p < 0.01$ vs ASE.

Figure 2. Specific antagonistic CL D1R suppresses anxiety-like behaviors and attenuates CaMKII^{CL} activation in ACE mice of adulthood. A, Experimental timeline and local injections of SCH-23390 in CL. Scale bar, 400/100 μm. **B**, EPM test. **C**, OFT. **D**, NSFT. **E,** The percentage and number of c-Fos-positive CaMKII^{CL} neurons. Scale bar, 100 μm. Vehicle, vehicle-treated ACE mice; SCH-23390, SCH-23390-treated ACE mice. N.S., $p > 0.05$, *, $p < 0.05$, **, $p < 0.01$ vs Vehicle.

Figure 3. Specific knockdown of CL D1R^{CaMKII} inhibits anxiety-like behaviors and attenuates CaMKII^{CL} activation in ACE of adulthood. A, Experimental design and timeline. **B**, Local injections of virus in CL. Scale bar, 300 μm. **C**, The D1R protein level in CL. **D**, EPM test. **E**, OFT. **F**, NSFT. **G**, The percentage and number of c-Fos-positive CaMKII^{CL} neurons. Scale bar, 400 μm/50 μm. ACE, adolescent cocaine exposure; ACE$_{Ctrl}$, ACE mice injected with control virus in CL; ACE$_{KD}$, ACE mice injected with knockdown virus in CL. N.S., $p > 0.05$, *, $p < 0.05$, **, $p < 0.01$ vs ACE$_{Ctrl}$.

Figure 4. EA treatment alleviates anxiety-like behaviors, rescues both CaMKII^{CL} activity and CL D1R^{CaMKII} levels in ACE mice of adulthood. A, Experimental design and timeline. **B**, EPM test. **C**, OFT. **D**, NSFT. **E**, The percentage and number of c-Fos-positive CaMKII^{CL} neurons. Scale bar, 300 μm/50 μm. **F**, The D1R protein level in CL. **G**, The staining of D1R^{CaMKII}. Scale bar, 200 μm/50 μm. **H**, Levels of p-ERK$_{1/2}$ and ERK$_{1/2}$ in CL. **I**, Levels of p-CREB, CREB and BDNF in CL. ACE$_{SEA}$, sham electro-acupuncture-treated

ACE mice; ACE_{EA}: electro-acupuncture (GV 20 and GV 29)-treated ACE mice. N.S., $p > 0.05$, *, $p < 0.05$, **, $p < 0.01$ vs ACE_{SEA}.

Figure 5. Graphical abstract. Adolescent cocaine exposure (ACE) enhances anxiety-like behaviors, activates more claustrum (CL) CaMKII-positive neurons ($CaMKII^{CL}$) and increases more expression of dopamine receptor 1 (D1R) on $CaMKII^{CL}$ ($D1R^{CaMKII}$) in mice of adulthood. Local blockade of CL D1R by SCH23390 or specific knockdown of CL $D1R^{CaMKII}$ by virus suppresses ACE-induced anxiety and $CaMKII^{CL}$ activity in mice of adulthood. Electroacupuncture (EA) at acupoints of GV20 and GV29 during withdrawal period efficiently reduces ACE-increased anxiety and $CaMKII^{CL}$ activity by targeting CL $D1R^{CaMKII}$ and its downstream signals including p-CREB and BDNF in mice of adulthood.

Figure 1

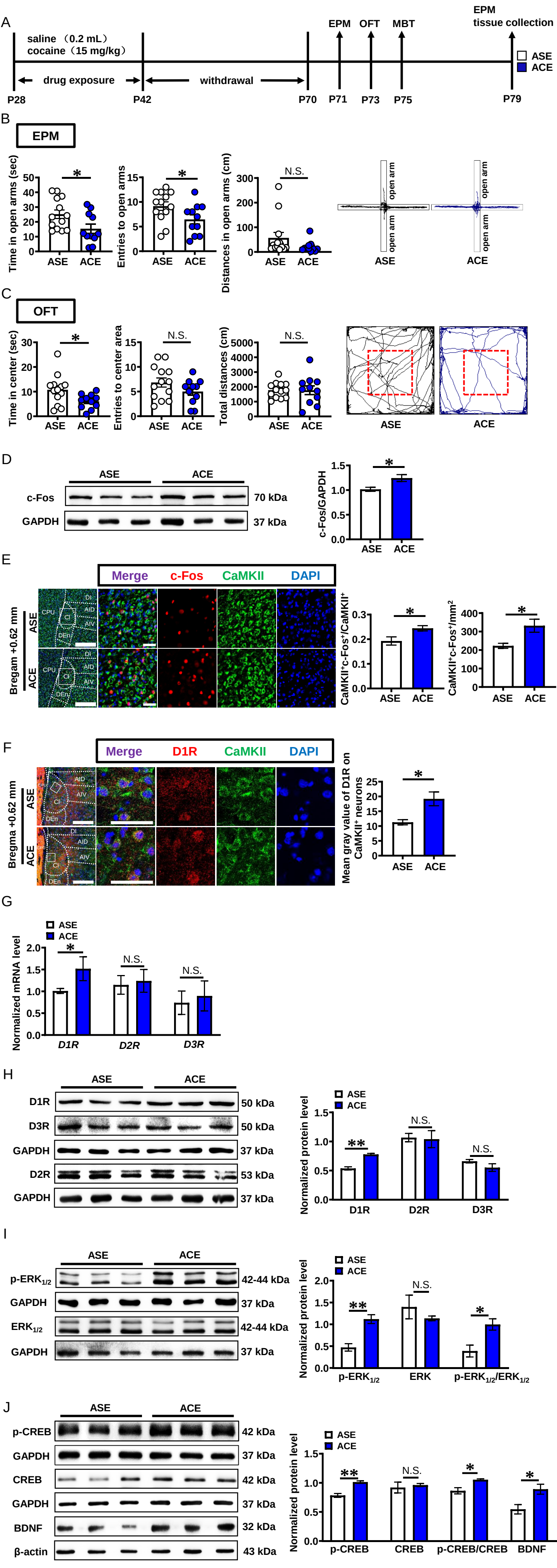
A
saline （0.2 mL）
cocaine（15 mg/kg）
drug exposure
withdrawal
P28
P42
P70
P71
P73
P75
P79
EPM
OFT
MBT
EPM
tissue collection
ASE
ACE
B
EPM
Time in open arms (sec)
Entries to open arms
Distances in open arms (cm)
N.S.
open arm
open arm
open arm
open arm
ASE
ACE
C
OFT
Time in center (sec)
Entries to center area
Total distances (cm)
N.S.
N.S.
ASE
ACE
D
ASE
ACE
c-Fos
GAPDH
70 kDa
37 kDa
c-Fos/GAPDH
E
Merge
c-Fos
CaMKII
DAPI
Bregam +0.62 mm
CPU
CI
DI
AID
AIV
DEn
CaMKII+c-Fos+/CaMKII+
CaMKII+c-Fos+/mm2
F
Merge
D1R
CaMKII
DAPI
Bregma +0.62 mm
Mean gray value of D1R on CaMKII+ neurons
G
Normalized mRNA level
D1R
D2R
D3R
H
D1R
D3R
GAPDH
D2R
GAPDH
50 kDa
50 kDa
37 kDa
53 kDa
37 kDa
Normalized protein level
I
p-ERK1/2
GAPDH
ERK1/2
GAPDH
42-44 kDa
37 kDa
42-44 kDa
37 kDa
p-ERK1/2
ERK
p-ERK1/2/ERK1/2
J
p-CREB
GAPDH
CREB
GAPDH
BDNF
β-actin
42 kDa
37 kDa
42 kDa
37 kDa
32 kDa
43 kDa
p-CREB
CREB
p-CREB/CREB
BDNF

Figure 2

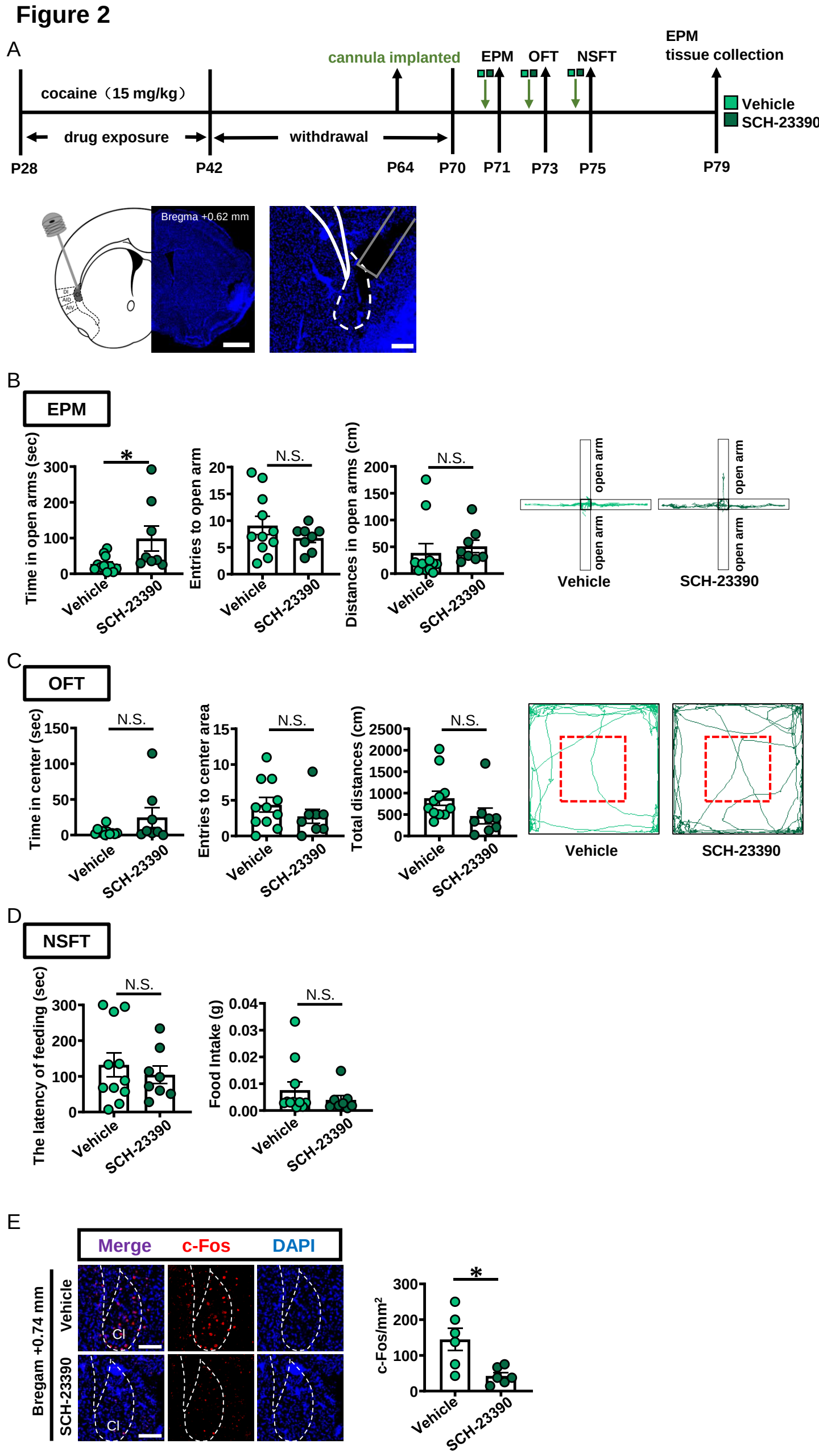
A
cannula implanted
EPM
OFT
NSFT
EPM
tissue collection
cocaine（15 mg/kg）
Vehicle
SCH-23390
drug exposure
withdrawal
P28
P42
P64
P70
P71
P73
P75
P79
Bregma +0.62 mm
B
EPM
Time in open arms (sec)
Entries to open arm
Distances in open arms (cm)
N.S.
*
Vehicle
SCH-23390
open arm
C
OFT
Time in center (sec)
Entries to center area
Total distances (cm)
D
NSFT
The latency of feeding (sec)
Food Intake (g)
E
Merge
c-Fos
DAPI
Bregam +0.74 mm
Cl
c-Fos/mm²

Figure 3

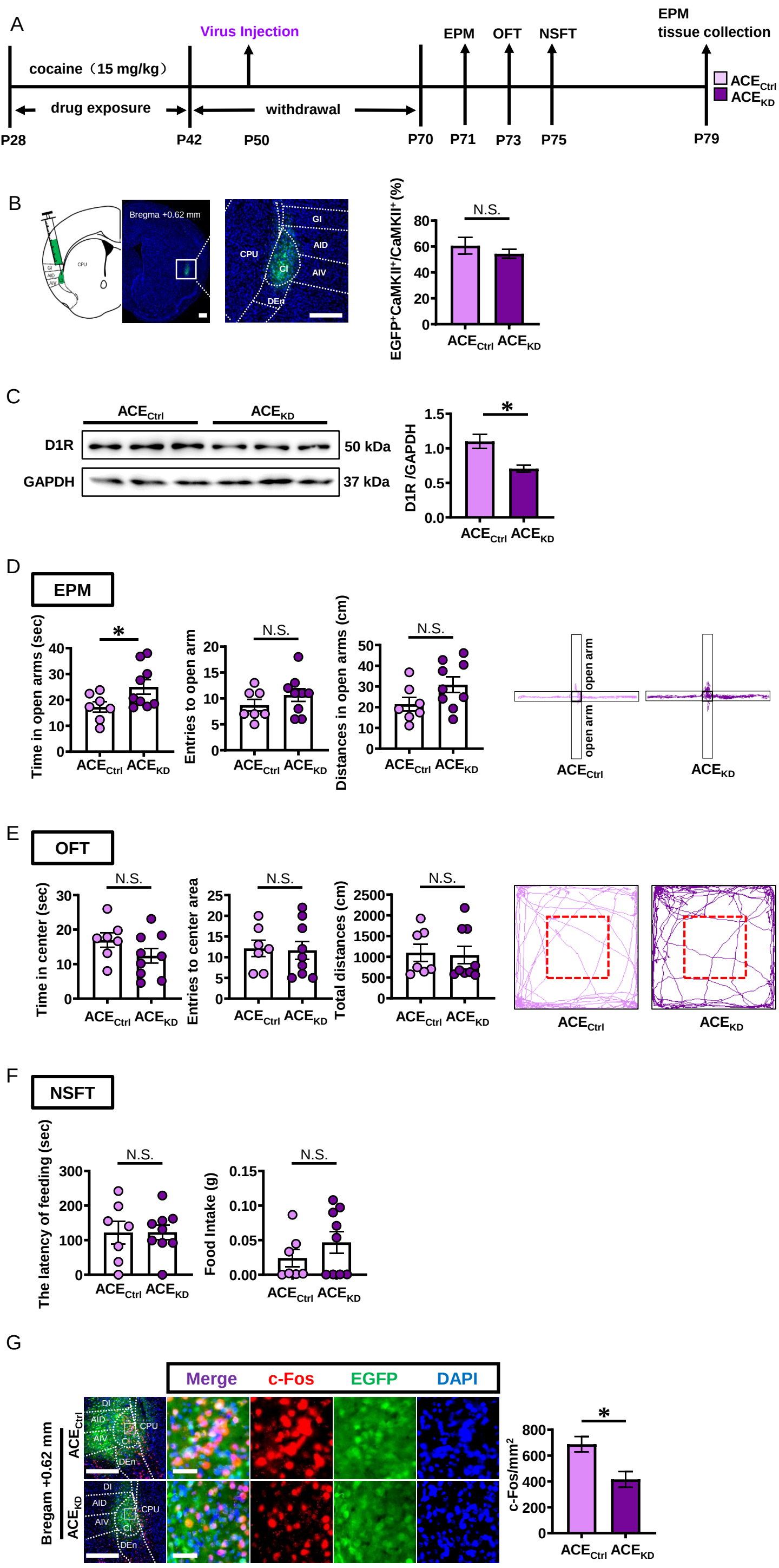
A
Virus Injection
EPM
OFT
NSFT
EPM
tissue collection
cocaine（15 mg/kg）
drug exposure
withdrawal
ACECtrl
ACEKD
P28
P42
P50
P70
P71
P73
P75
P79
B
Bregma +0.62 mm
CPU
GI
AID
AIV
CI
DEn
N.S.
EGFP+CaMKII+/CaMKII+ (%)
ACECtrl ACEKD
C
ACECtrl
ACEKD
D1R
GAPDH
50 kDa
37 kDa
D1R /GAPDH
*
D
EPM
Time in open arms (sec)
Entries to open arm
Distances in open arms (cm)
open arm
open arm
E
OFT
Time in center (sec)
Entries to center area
Total distances (cm)
F
NSFT
The latency of feeding (sec)
Food Intake (g)
G
Merge
c-Fos
EGFP
DAPI
Bregam +0.62 mm
c-Fos/mm2

Figure 4

A

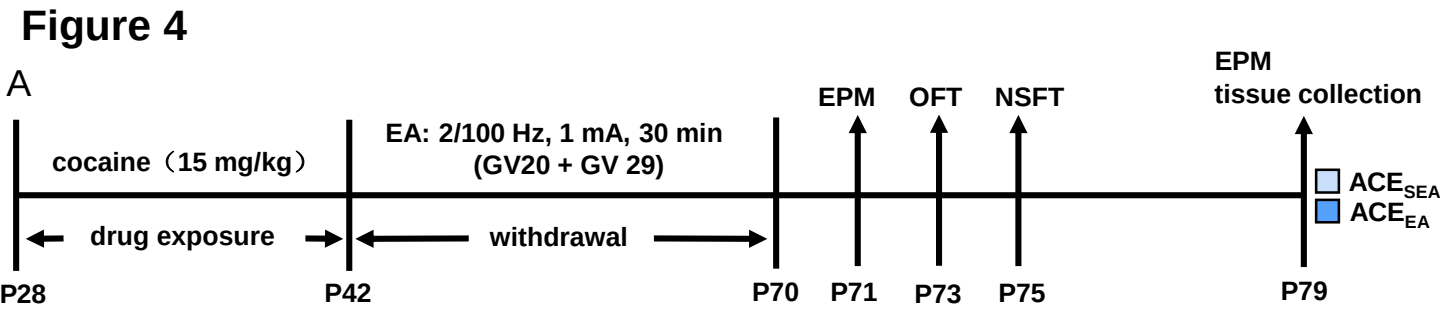

B

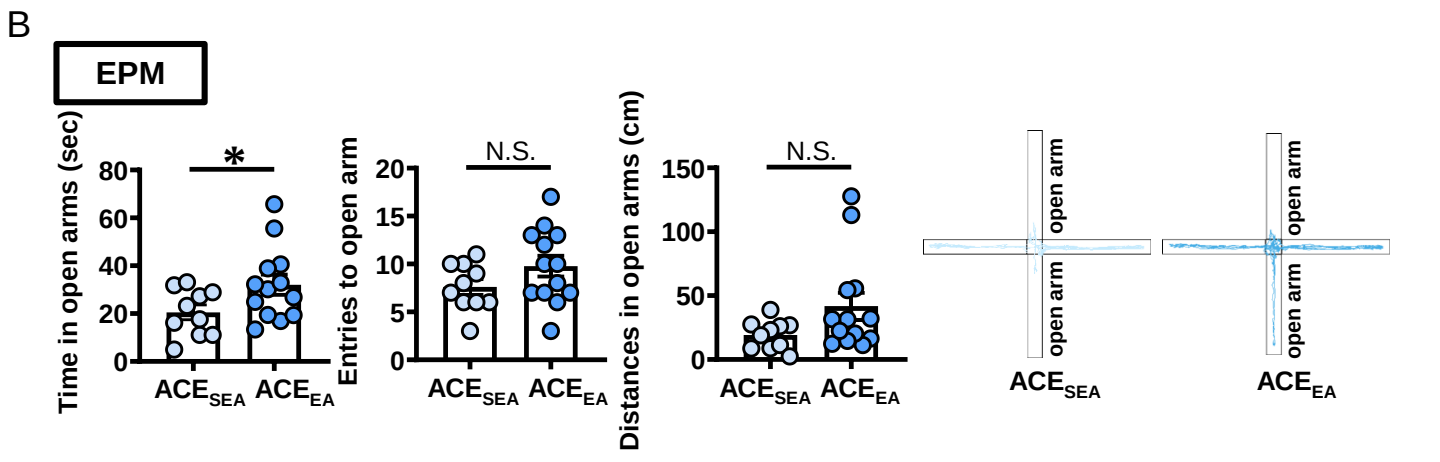

C

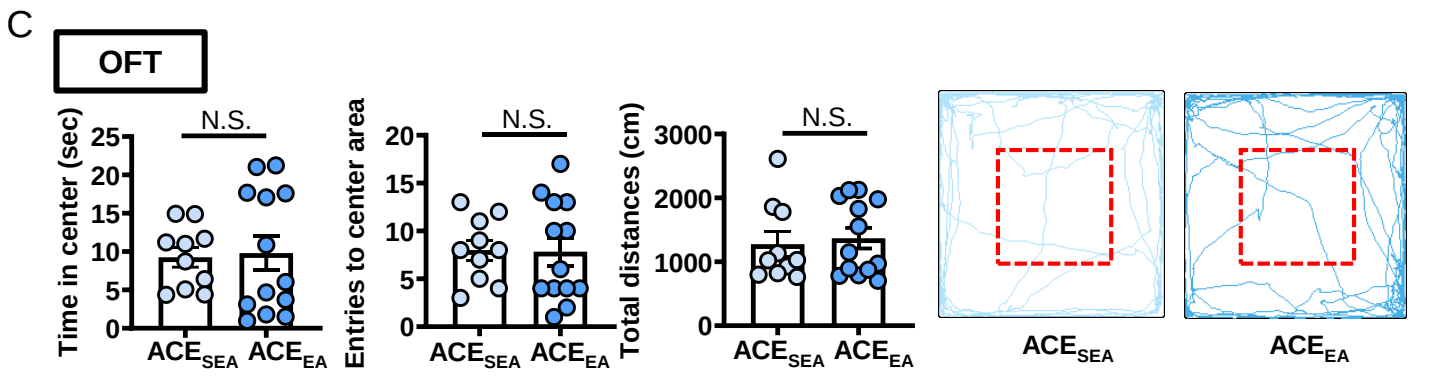

D

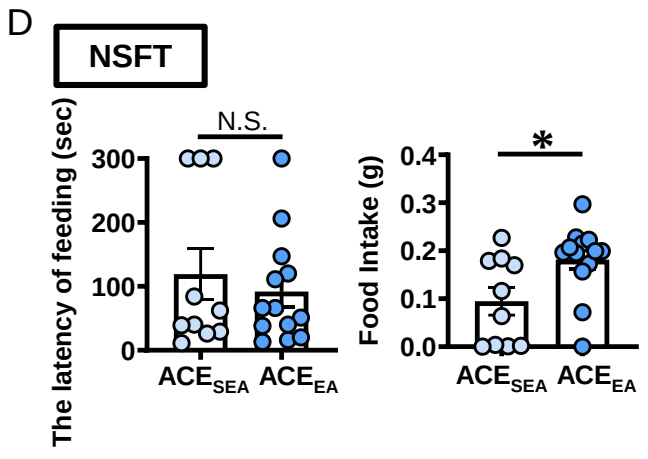

E

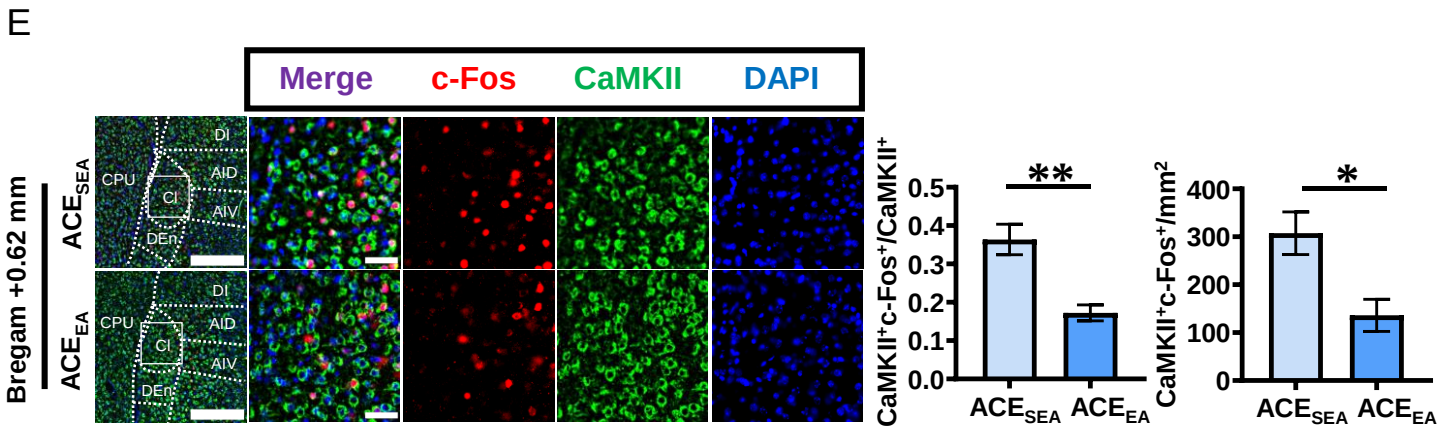

F

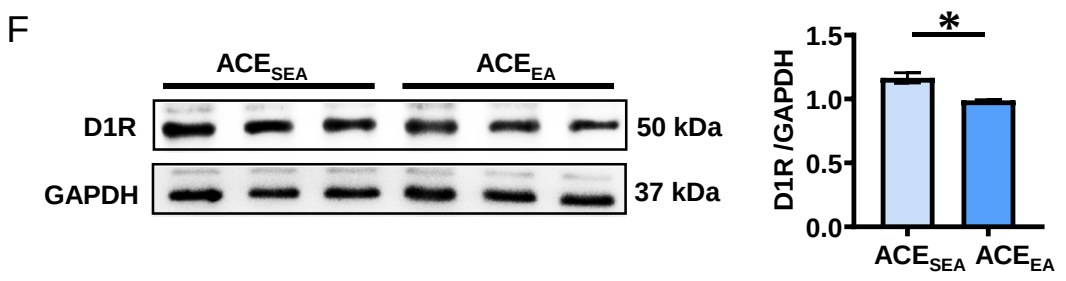

G

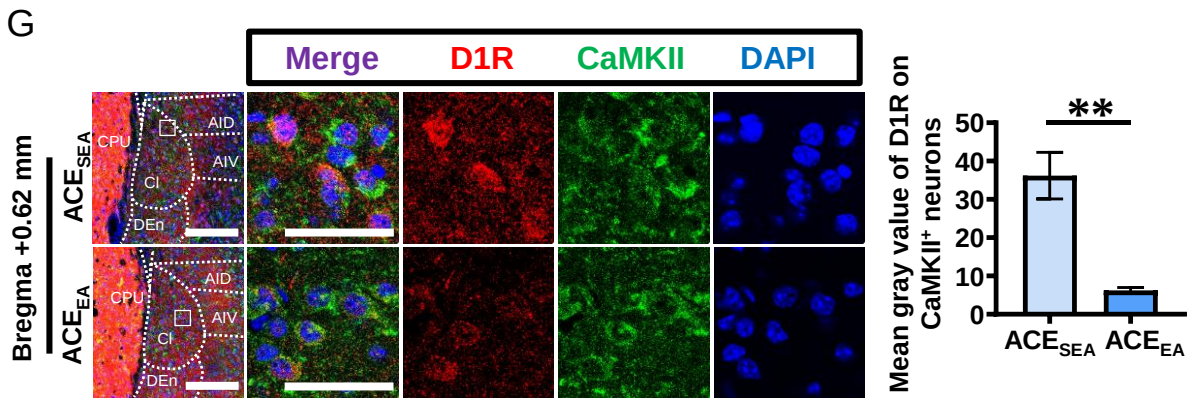

H

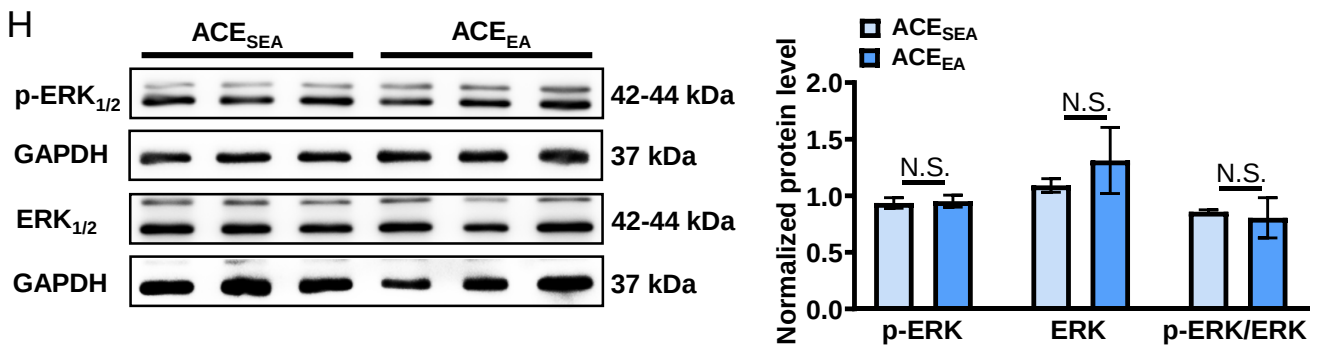

I

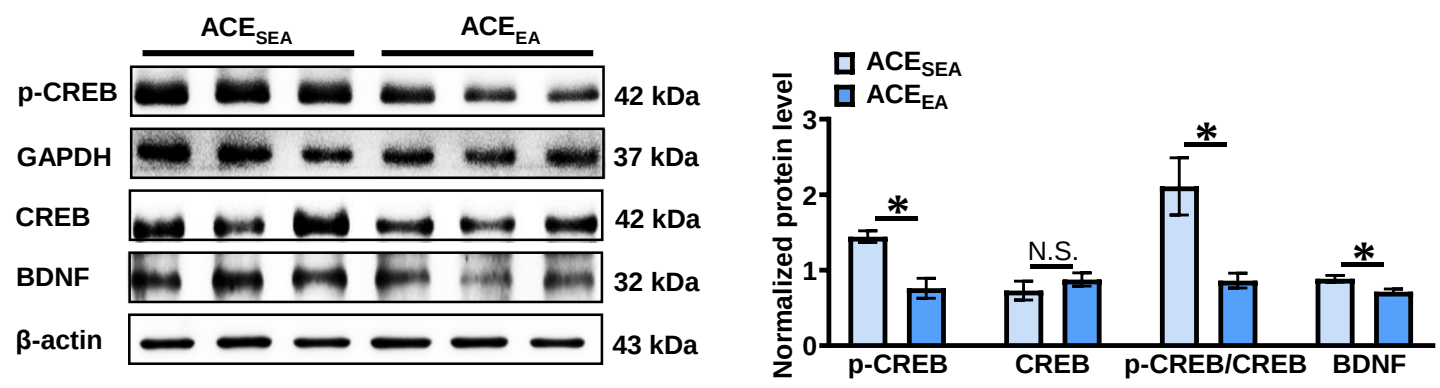

Figure 5

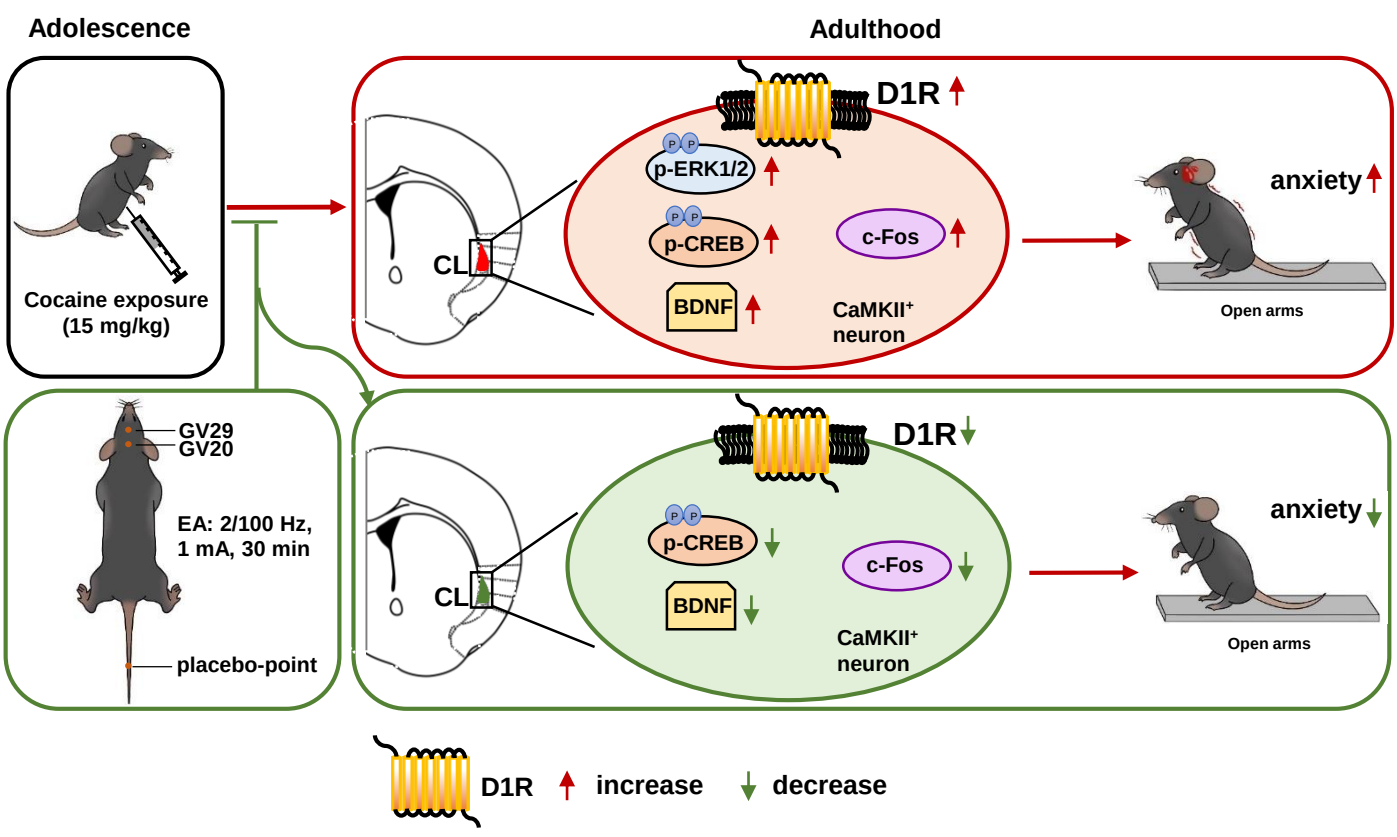
Adolescence
Adulthood
Cocaine exposure
(15 mg/kg)
D1R
p-ERK1/2
p-CREB
c-Fos
BDNF
CL
CaMKII+
neuron
anxiety
Open arms
GV29
GV20
EA: 2/100 Hz,
1 mA, 30 min
placebo-point
D1R
p-CREB
c-Fos
BDNF
CL
CaMKII+
neuron
anxiety
Open arms

D1R
increase
decrease

Supplementary Data

Figure legends

Figure S1. The MBT in adult mice. ASE, adolescent saline exposure; ACE, adolescent cocaine exposure. N.S., $p > 0.05$ vs ASE.

Figure S2. The schematic diagram of acupoint GV20 and GV29. A, Schematic diagram of EA and SEA treatments in mice. ACE, adolescent cocaine exposure; ACE_{SEA}, sham electro-acupuncture-treated ACE mice; ACE_{EA}, electro-acupuncture (GV20 and GV29)-treated ACE mice.

Figure S1

A

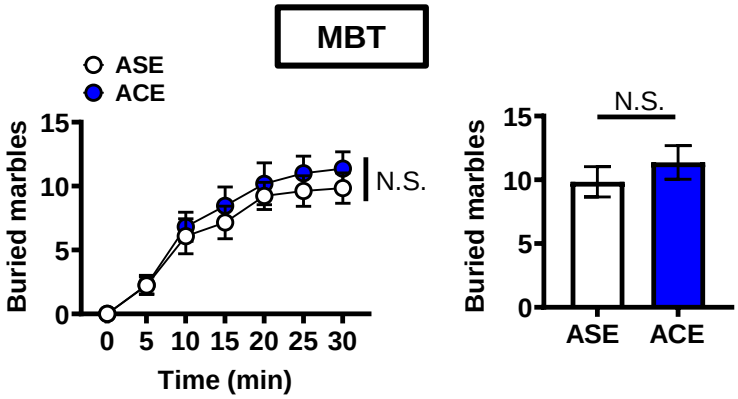
MBT
ASE
ACE
Buried marbles
15
10
5
0
0 5 10 15 20 25 30
Time (min)
N.S.
N.S.
Buried marbles
15
10
5
0
ASE
ACE

Figure S2

A

ACE_{SEA} **ACE_{EA}**